Development of a Rapid Point-Of-Care Test that Measures Neutralizing Antibodies to SARS-CoV-2

Douglas F. Lake[1*#], Alexa J. Roeder[1*], Erin Kaleta[2], Paniz Jasbi[3], Sivakumar Periasamy[4,5] Natalia Kuzmina[4,5] Alexander Bukreyev[4,5,6], Thomas Grys[2], Liang Wu[7], John R Mills[7], Kathrine McAulay[2], Maria Gonzalez-Moa[8], Alim Seit-Nebi[8], and Sergei Svarovsky[8]

Affiliations:

1. School of Life Sciences, Arizona State University, Tempe AZ, USA
2. Mayo Clinic Arizona, Department of Laboratory Medicine and Pathology, Scottsdale, AZ, USA
3. College of Health Solutions, Arizona State University, Phoenix AZ, USA
4. Department of Pathology, University of Texas Medical Branch at Galveston, Galveston, TX USA
5. Galveston National Laboratory, University of Texas Medical Branch at Galveston, Galveston, TX USA
6. Department of Microbiology and Immunology University of Texas Medical Branch at Galveston, Galveston, TX USA
7. Mayo Clinic Rochester, Department of Laboratory Medicine and Pathology, Rochester, MN USA
8. Axim Biotechnologies Inc, San Diego, CA USA

*Co-first authors

Running Head: Rapid Neutralization Test for COVID-19

#Address correspondence to Douglas F. Lake, douglas.lake@asu.edu

Douglas F Lake and Alexa J Roeder contributed equally to this work. Author order was determined on the basis of seniority

Abstract:

As increasing numbers of people recover from and are vaccinated against COVID-19, tests are needed to measure levels of protective, neutralizing antibodies longitudinally to help determine duration of immunity. We developed a lateral flow assay (LFA) that measures levels of neutralizing antibodies in plasma, serum or whole blood. The LFA is based on the principle that neutralizing antibodies inhibit binding of the spike protein receptor-binding domain (RBD) to angiotensin-converting enzyme 2 (ACE2). The LFA compares favorably with authentic SARS-CoV-2 and pseudotype neutralization assays with an accuracy of 98%. Sera obtained from patients with seasonal coronaviruses did not prevent RBD from binding to ACE2. To demonstrate the usefulness of the LFA for measuring antibodies in convalescent plasma used for therapy, we measured conversion of non-immune plasma into strongly neutralizing plasma. This is the first report of a neutralizing antibody test that is rapid, highly portable and relatively inexpensive that might be useful in assessing COVID-19 vaccine-induced immunity.

Introduction

The pandemic virus, Severe Acute Respiratory Syndrome Coronavirus-2 (SARS-CoV-2) continues to be transmitted by person to person spread from its origin in Wuhan, China in December 2019(1–3) . Vaccine trials are ongoing, and preliminary results from at least 2 vaccines show that the vaccines elicit protective immunity, but durability of vaccine responses is not known(4).

Molecular tests such as PCR detect SARS-CoV-2 nucleic acid in nasopharyngeal secretions and saliva and are diagnostic of infection(5). These molecular tests can determine the rate of infection and potential re-infection. When negative they indicate that patients have cleared the virus. In response to infection, all immunocompetent hosts generate antibodies against the virus. Patients may have a positive serologic test result as well as a PCR-positive

test result if they are early in convalescence(6). For SARS-CoV-2, antibodies to spike protein do not always predict recovery from COVID-19(7).

Although immunocompetent individuals infected with SARS-CoV-2 generate antibodies against the virus, it is essential to know which individuals generate high levels of neutralizing antibodies (NAbs) so that they can resume normal activities without fear of being re-infected and spreading the virus to others(8–10). The goal of COVID-19 vaccines is to induce NAbs and T cell responses that prevent infection/re-infection. Additionally, development of NAbs indicates which individuals might be optimal donors for convalescent plasma protocols. Although NAbs are important for elimination of the virus and protection from subsequent infection, it has been reported by several groups that up to one-third of convalescent plasma samples from individuals who have recovered from COVID-19 do not neutralize SARS-CoV-2 or spike pseudotype virus infection(11–13).

Viral neutralization assays measure levels of antibodies that block infection of host cells. Two main types of viral neutralization assays are utilized for SARS-CoV-2. Authentic microneutralization assays measure reduction of viral plaques or infectious foci in microneutralization assays in susceptible host cells using SARS-CoV-2 under BSL3 conditions. These assays are slow, laborious, require highly trained personnel and require a BSL3 facility. Pseudotype virus neutralization assays have been developed in which SARS-CoV-2 spike protein is expressed in a virus such as vesicular stomatitis virus or lentivirus(14, 15). These assays are faster and less dangerous than authentic microneutralization assays, but still require BSL2 conditions and 24-48 hours for results. Another challenge is that both authentic and pseudovirus virus neutralization assays depend on host cells for infection which adds variability to the assay.

It is known that SARS-CoV-2 uses receptor binding domain (RBD) on spike protein to bind angiotensin converting enzyme 2 (ACE2) on host cells; this appears to be the principal

neutralizing domain of SARS-CoV-2(16, 17). Using this knowledge, we developed a lateral flow assay (LFA) that measures levels of (neutralizing) antibodies which block RBD from binding to ACE2. Other groups have developed RBD-ACE2-based competition ELISAs(18)-(19) but none have developed a rapid, highly portable semi-quantitative point-of-care (POC) test.

Methods

Human Subjects and Samples

Peripheral blood, serum and plasma were collected for this study under an Arizona State University institutional review board (IRB) approved protocol #0601000548 and Mayo Clinic IRB protocol #20-004544. Plasma was obtained by ficoll gradient separation of peripheral blood and serum was obtained by centrifugation 30 minutes after drawing blood. Plasma and serum samples obtained from excess clinical samples at Mayo Clinic were pre-existing, de-identified and leftover from normal workflow. COVID-19 samples ranged from 3 to 84 days post PCR positive result. Residual clinical samples were stored at 2-8^{o}C for up to 7 days, and frozen at -80^{o}C thereafter.

Serum samples from patients with non-COVID-19 respiratory illnesses were also tested. These specimens were collected from patients from 2/14/17 – 4/6/20 and were tested by the FilmArray Respiratory Panel 2 (RP2) (Biofire Diagnostics, Salt Lake City, UT) respiratory virus panel as part of routine clinical workflow. Specimens were stored at -80°C until analysis.

Pseudotype Virus Neutralization Assays

Titers were obtained from 60 COVID-19 patient sera using a vesicular stomatitis virus (VSV) spike protein pseudotype assay as previously reported with modifications (14). Patient sera had been stored at -80°C prior to testing. Briefly, SARS-CoV-2 pseudotypes were created by replacing VSV G glycoprotein with SARS-CoV-2 spike protein resulting in a pseudotyped virus with the C-terminal 19 amino acids removed from spike. The pseudotyped virus is called VSV-

SARS-CoV-2-S-Δ19CT and was produced by BHK-21 cells. It induces syncytium formation when incubated with vero cells. Two different Vero cells encoding split product luciferase (DSP1 and DSP2) were cultured at a 1:1 ratio as a monolayer. Virus-induced fusion leads to luciferase complementation and in the presence of luciferase substrate EnduRen™ (Promega, Madison, WI) generates luminescence. The higher luminescence, the more infection events by the virus. A human monoclonal antibody (Regeneron, Tarrytown, NY) targeting the SARS-CoV-2 spike protein was diluted to set a cut-off at 50% neutralizing activity and utilized as a single point calibrator. Patient sera with serial dilutions (1:80-1:2560) and the calibrator were pre-incubated with virus for 30 minutes (neutralization) prior to addition to DSP1 and DSP2 Vero cells. The virus-cell mixture was incubated at 37°C in a 5% $C0_2$ incubator for a total of 24 hours before luminescence reading; the substrate EnduRen™ was added at 18 hours of incubation. The raw luminescence signal of each sera dilution was compared against the raw luminescence signal of the calibrator. The last consecutive dilution with luminescence signal below the calibrator was considered the end-point titer. Samples were tested in duplicate. The same serum samples, 68 coded sera (10 serum samples at titers of 1:80, 1:160, 1:320, 1:640, 1:1280, 1:2560 and 8 serum samples from individuals never infected with COVID-19) were frozen at -20ºC and shipped by Dr. Mills from Mayo Clinic Rochester to Mayo Clinic Arizona and the Lake Lab for LFA testing.

Authentic SARS-CoV-2 Microneutralization Assay

The authentic microneutralizing assay was performed using a recombinant SARS-CoV-2 that expresses mNeonGreen (SARS-CoV-2ng) during replication in permissive cells, as previously described (20). Inhibitory concentrations for which 50% of virus is neutralized by serum antibodies (IC_{50} values) were obtained on a unique set of 38 COVID-19 sera. Sixty µl aliquots of SARS-CoV-2ng were pre-incubated for 1 h in 5% CO_2 at 37ºC with 60µl serial 2-fold serum

dilutions in cell culture media, and 100µl were inoculated into Vero-E6 monolayers in black polystyrene 96-well plates with clear bottoms (Corning, Tewksbury, MA). Each serum was tested in duplicates. The final amount of the virus was 200 PFU/well, and the starting serum dilution was 1:20 and the end dilution was 1280 unless an IC_{50} was not reached in which case serum was diluted to 1:10240. Cells were maintained in Minimal Essential Medium (ThermoFisher Scientific, Waltham, MA) supplemented by 2% FBS (HyClone, Logan, UT) and 0.1% gentamycin in 5% CO_2 at 37ºC. After 2 days of incubation, fluorescence intensity of infected cells was measured at a 488 nm wavelength using a Synergy 2 Cell Imaging Reader (Biotek, Winooski, VT). The signal readout was normalized to virus control aliquots with no serum added and was presented as the percentage of neutralization. IC_{50} was calculated with GraphPadPrism 6.0 software. Work with infectious SARS-CoV-2ng was performed in a BSL-3 biocontainment laboratory of the University of Texas Medical Branch, Galveston, Tx, Galveston National Laboratory.

Serologic Antibody Assay

The Ortho Vitros Anti-SARS-CoV-2 IgG test was performed on the Ortho Clinical Diagnostics Vitros 3600 Immunodiagnostics System (Ortho, Raritan, NJ) following manufacturer's instructions at the Mayo Clinic. This assay is approved for use in clinical testing under FDA Emergency Use Authorization to qualitatively detect antibody to the S1 subunit of SARS-CoV-2 spike protein. Results are reported as reactive (S/CO ≥ 1.0) or Nonreactive (S/CO <1.0). Quantitative results are not reported for clinical workflows but are measured and recorded in this assay. Specimens were tested within 7 days of collection and were stored at 2-8^{o}C per manufacturer's instructions. This assay was performed after the VSV assay was performed on the set of 60 serum samples, then the samples were frozen at -80°C before running them on the LFA. A separate set of 38 samples was run concurrently in the SARS-CoV-2 authentic microneutralizing antibody assay, the LFA, and the Ortho Vitros Anti-SARS-CoV-2 IgG assay.

Lateral Flow Neutralizing Antibody Assay

The Lateral Flow Neutralizing Antibody assay was developed to detect antibodies that compete with ACE2 for binding to RBD. The LFA cassette contains a test strip composed of a sample pad and blood filter, conjugate pad, nitrocellulose membrane striped with test and control lines, and an absorbent pad to wick excess moisture (Axim Biotechnologies Inc, San Diego, CA). The blood filter allows serum to pass through but prevents red blood cells and leukocytes from interfering with the assay. Test strips are secured in a cassette that contains a single sample port (Empowered Diagnostics, Pompano Beach, FL). For procedural control purposes, the LFA also contains a control mouse antibody conjugated to red gold nanospheres and corresponding anti-mouse control line.

LFAs were performed at ambient temperature and humidity on a dry, flat surface and left to run undisturbed for 10 minutes prior to reading results. First, 10µl of plasma, serum or whole blood were transferred to the cassette sample port and immediately followed by two drops (~50µl) of chase buffer. After 10 minutes, each test was placed in an iDetekt RDS-2500 LFA reader (Austin, TX) and the densities of both test and control lines were recorded electronically. This assay was performed on the VSV subset (n = 60) as well as the authentic SARS-CoV-2 microneutralizing antibody assay subset (n = 38).

Serum samples from COVID-19 patients as well as sera from patients with PCR-confirmed seasonal respiratory viruses including PCR-confirmed seasonal coronaviruses were tested in the LFA as controls. Twenty-seven sera from patients with seasonal respiratory viruses were tested in the LFA in a manner identical to COVID-19 sera.

The test leverages the interaction between RBD-conjugated green-gold nanoshells (Nanocomposix, San Diego, CA) that bind ACE2 at the test line when RBD-binding/neutralizing

antibodies (RBD-NAbs) are absent or low. As indicated by the competitive nature of this assay, test line density is inversely proportional to RBD-NAbs present within the sample. Thus, an absent or faint test line indicates high levels of RBD-NAbs, whereas a dark or strong test line suggests lack of RBD-NAbs within a given plasma sample (Figure 1A).

As a semi-quantitative test, the results of the LFA can be interpreted using a scorecard or a densitometer. Figure 1B demonstrates the scorecard. Red control line across from the "C" on the cassette is composed of a mouse monoclonal antibody coupled to red-gold beads binding to an anti-mouse IgG. A red line indicates that the test ran properly and the green test line across from the "T" can be used to semi-quantitatively measure the ability of plasma, serum or whole blood to block RBD on green-gold nanoshells from binding to ACE2.

To demonstrate the ability of the test to measure NAbs in whole blood, 10μg of a neutralizing monoclonal antibody (mAb) based on the sequence of B-38(20)(Axim Biotechnologies, Inc, San Diego, CA) was mixed with 10μl of normal donor whole blood collected in a heparinized blood collection tube. Two-fold dilutions were made in whole blood to a final concentration of 0.625μg/ml neutralizing mAb. Then, 10μl of each dilution were transferred to LFA cassettes, chased with 50μl running buffer, and read with an LFA reader after 10 minutes.

Conversion of Non-immune Normal Human Plasma (NIHP) into Neutralizing Plasma

To convert NIHP into strongly neutralizing plasma (SNP), plasma from a convalescent donor who demonstrated the ability to block RBD from binding to ACE2 (M21) was mixed with NIHP collected prior to December 2019. For example, for a 1% mixture, 1μl of SNP was mixed with 99μl NIHP; for a 5% mixture 5μl of SNP was admixed with 95μl NIHP, etc. We performed the test with 10μl of 1%, 5%, 10%, and 20% SNP admixed into NIHP.

208 *Data Analysis*

209 Pearson's correlation (*r*) was conducted to assess the strength and significance of
210 associations between the LFA, the Ortho Vitros Anti-SARS-CoV-2 IgG test, VSV titers and IC_{50}
211 values. Regression analysis using IC_{50} values was performed to evaluate consistency(18) while
212 Bland-Altman plots were constructed to assess agreement and bias(21, 22). Correlation analysis
213 was conducted using IBM SPSS (Armonk, NY). Regression analysis was performed using
214 Microsoft Excel (Redmond, WA); Bland-Altman plots were visualized using IBM SPSS. For two-
215 group analysis, IC_{50} values corresponding to >240 were categorized as titer of ≥1:320
216 (neutralizing), whereas IC_{50} values ≤240 were categorized as ≤1:160 (non-neutralizing). Receiver
217 operating characteristic (ROC) analysis was performed to assess classification accuracy,
218 sensitivity, and specificity of the LFA and Ortho Vitros Anti-SARS-CoV-2 IgG test methods in
219 assessing neutralizing capacity; optimal cutoffs for each method were established to maximize
220 area under curve (AUC)(23, 24). ROC analysis was conducted using R language in the RStudio
221 environment (version 3.6.2; RStudio PBC, Boston, MA). All analyses were conducted using raw
222 values; data were not normalized, transformed, or scaled.
223
224 **Results**
225 The lateral flow assay reported here is a rapid 10-minute POC test. As shown in the
226 schematic in **Figure 1A**, this test utilizes serum, plasma or whole blood to semi-quantitatively
227 measure levels of NAbs. An example of strong, moderate and non-neutralizing sera is shown in
228 **Figure 1B**. As diagrammed in **Figure 1A**, levels of NAbs in serum or plasma are reflected by
229 the intensity of the test line which can be read on a hand-held densitometer or compared
230 visually to a scorecard (**Figure 1B)**. Strong neutralization results in a weak line because
231 neutralizing antibodies are binding RBD on green gold beads and preventing RBD-beads from
232 binding to the ACE2 cellular receptor at the test line.
233

234

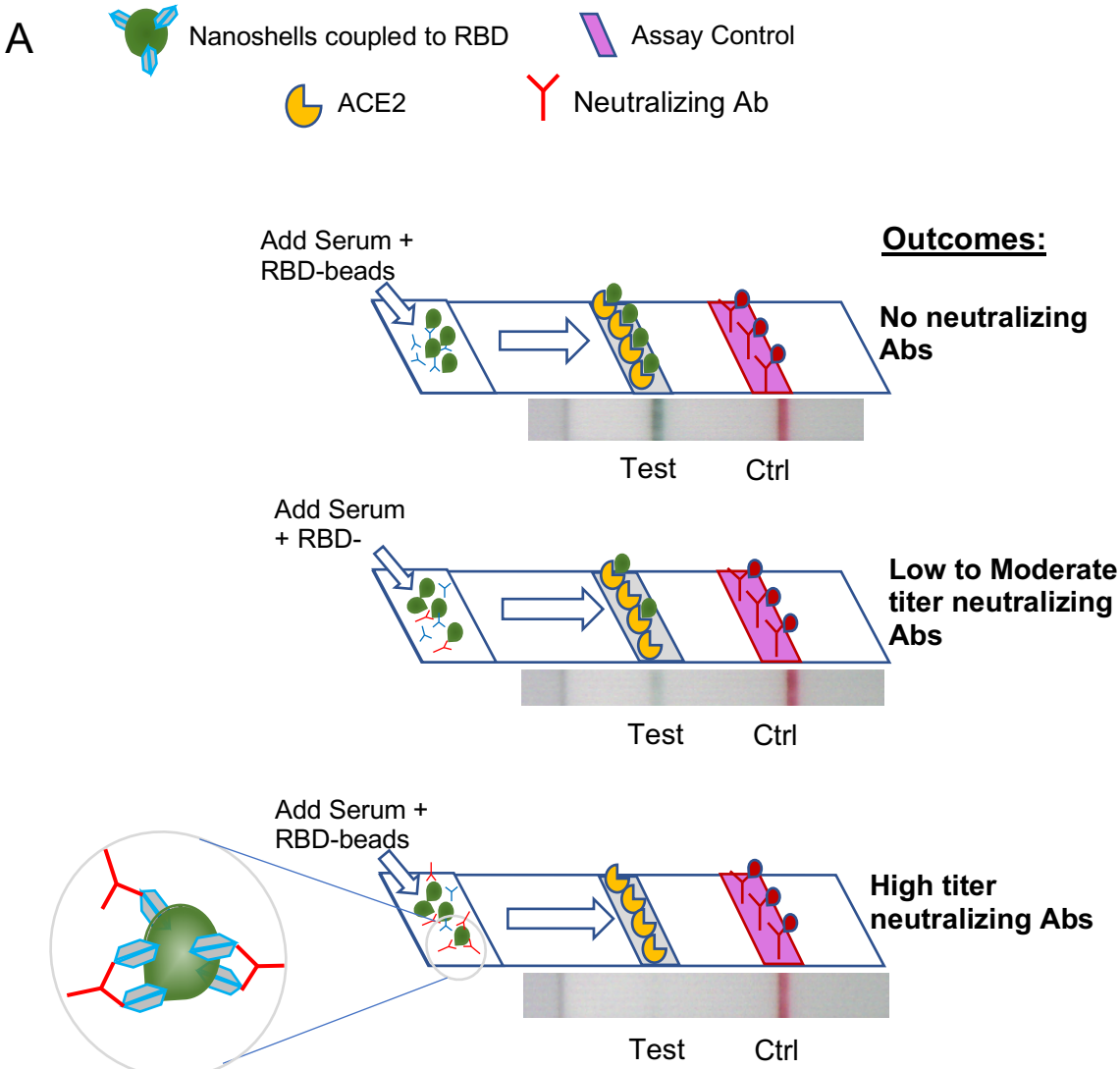

235
236
237
238

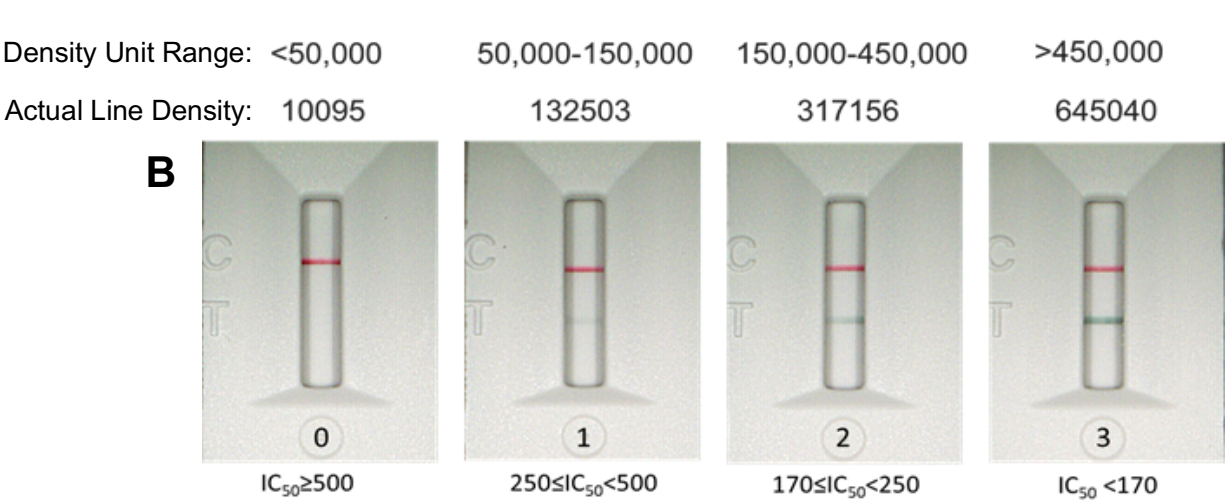

Figure 1.
(A) Schematic of Neutralization LFA. Below each graphic is a representative image of a lateral flow strip demonstrating actual line density. Addition of non-COVID19-immune serum or plasma (*top*) does not block binding of RBD-beads (green particles) to ACE2 resulting in the RBD-bead–ACE2 complex creating a visible line. Addition of patient serum with moderate titer NAbs to the sample pad creates a weak line (*middle*). Addition of patient serum with high titer NAbs (> 1:640) blocks binding of RBD-beads to ACE2 such that no line is observed at the test location on the strip (*bottom*). Red control line represents capture of a mouse monoclonal antibody coupled to red beads. **(B)** Scorecard for measuring levels of NAbs . Red control line across from the "C" on the cassette indicates that the test ran properly and the green test line across from the "T" can be used to measure the ability of plasma or serum to block RBD on gold nanoshells from binding to ACE2. **(0)** represents patient serum producing a visually non-existent line with density units of 10,095 and an IC_{50}>500 (IC_{50}=1151); **(1)** represents patient serum with a line density of 132,503 and an IC_{50} of 396; **(2)** represents patient serum with a line density of 239,987 and an IC_{50} of 243; (**3)** represents patient serum with a line density of 485,665 and an IC_{50} of 96.

We tested 60 serum samples with known neutralization titers obtained in a VSV-based spike pseudotype assay in our LFA. De-identified serum samples were sent from Mayo Clinic Rochester to our laboratories at Mayo Clinic Arizona and run in a blinded manner. The LFA result compared favorably with serum titers, especially at higher titers and correctly distinguished all eight non-neutralizing serum samples (**Figure 2A**).

To further support the application of our lateral flow test to measure levels of antibodies that neutralize SARS-CoV-2, we tested a different set of 38 serum samples that were assigned IC_{50} values in an authentic SARS-CoV-2 microneutralization assay(25). Again, the experiment was performed in a blinded manner such that personnel running either the LFA or the microneutralization assay did not know the results of the comparator test. When line densities from the LFA were plotted against IC_{50} values determined in the SARS-CoV-2 microneutralization

assay, serum samples with strong neutralization activity demonstrated low line densities; this indicates that neutralizing antibodies inhibited RBD from binding to ACE2 (**Figure 2B**).

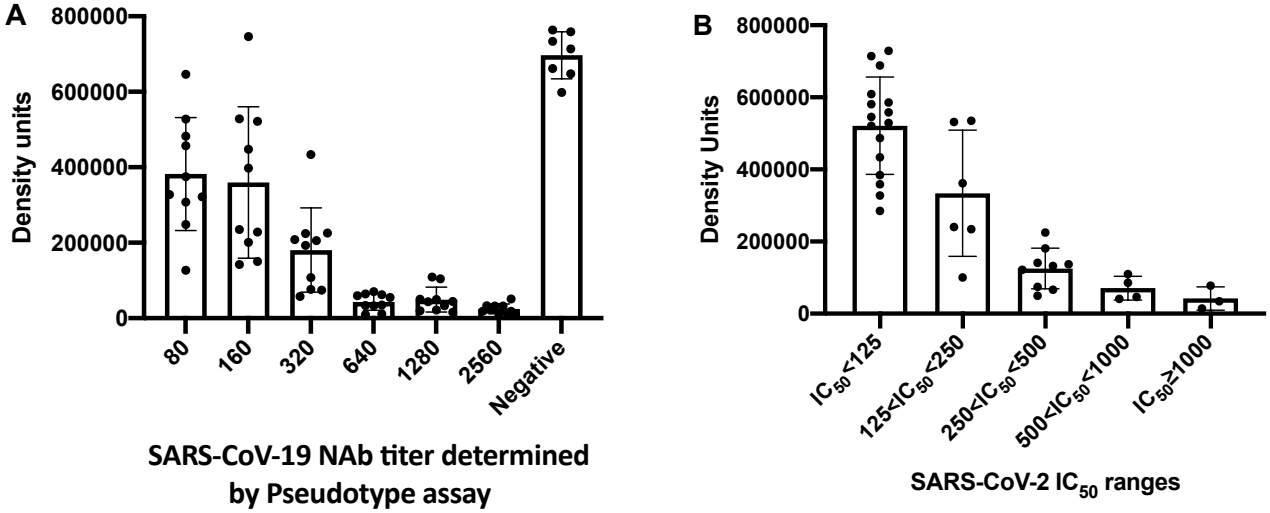

Figure 2. (A) Comparison of RBD-ACE2 competition LFA Density Units with VSV-Spike pseudotype virus assay titers using 60 convalescent serum samples. Titers from the pseudotype assay are shown on the X-axis. Scatter plots with bar graph including standard deviation of the mean for 10 serum samples at each titer except for negative donor serum which is eight samples. **(B)** Comparison of RBD-ACE2 competition LFA with IC_{50} values determined in a SARS-CoV-2 microneutralization assay on 38 samples (collected 3 to 90 days after PCR positive result). Ranges of IC_{50} values are shown on the X-axis plotted against LFA line density units on the Y-axis.

Next, we determined if our test detected any neutralization activity in serum samples collected from patients with other PCR -confirmed respiratory viruses including seasonal coronaviruses (**Figure 3A**) and for serum samples collected prior to December 2019 (**Figure 3B).** None of the seasonal respiratory virus plasma samples, including pre-December 2019 samples showed neutralizing activity.

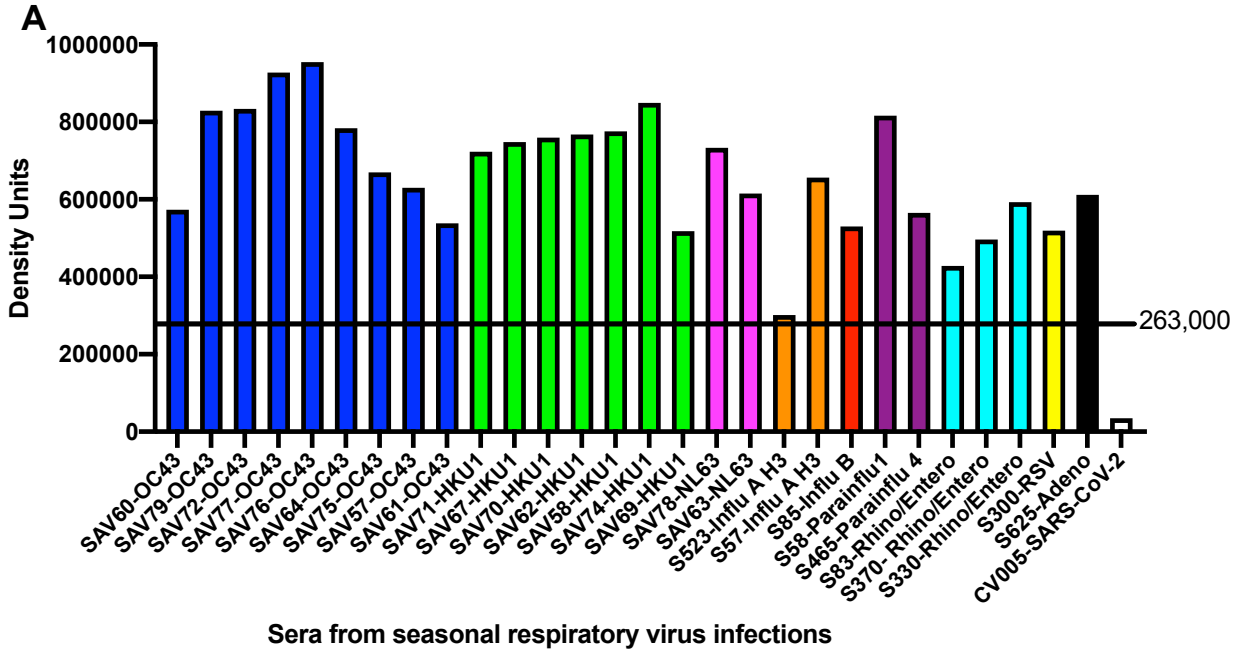

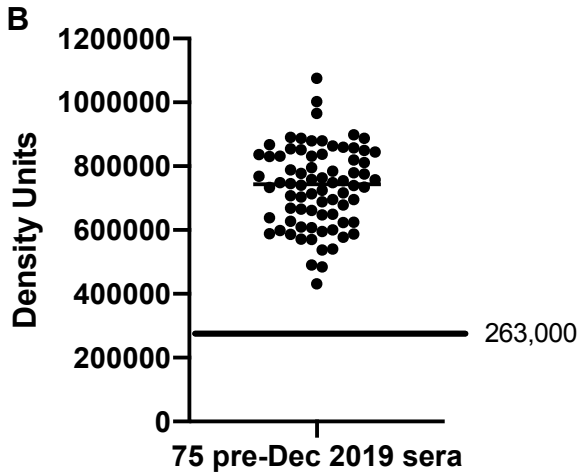

Figure 3. A) Serum samples collected with PCR-confirmed diagnosis of seasonal respiratory viruses (Coronavirus OC43, blue; Coronavirus HKU-1, green; Coronavirus NL-63, pink; influenza A, orange, influenza B, red ; parainfluenza, purple ; rhinovirus, teal ; respiratory syncycial virus, yellow ; and adenovirus, black were run on the LFA as described in Methods.

A positive control serum from a convalescent COVID-19 patient is shown on the far right of the bar graph in white. **B)** Serum samples collected pre-December 2019. Cutoff value of 263,000 density units was calculated based on receiver operating characteristic curves (see Figure 6).

We evaluated how the Ortho Vitros Anti-SARS-CoV-2 IgG test and our LFA compared to IC_{50} values determined in an authentic SARS-CoV-2 microneutralization assay using 38 COVID-19 sera. FDA guidance indicates that an Ortho Vitros Anti-SARS-CoV-2 IgG test of ≥12 meets a threshold for convalescent plasma use in patients with COVID-19. To determine the agreement between our lateral flow assay and the Ortho Vitros Anti-SARS-CoV-2 IgG test, density units from our LFA and values from the Ortho test were regressed onto IC_{50} values (**Figure 4**).

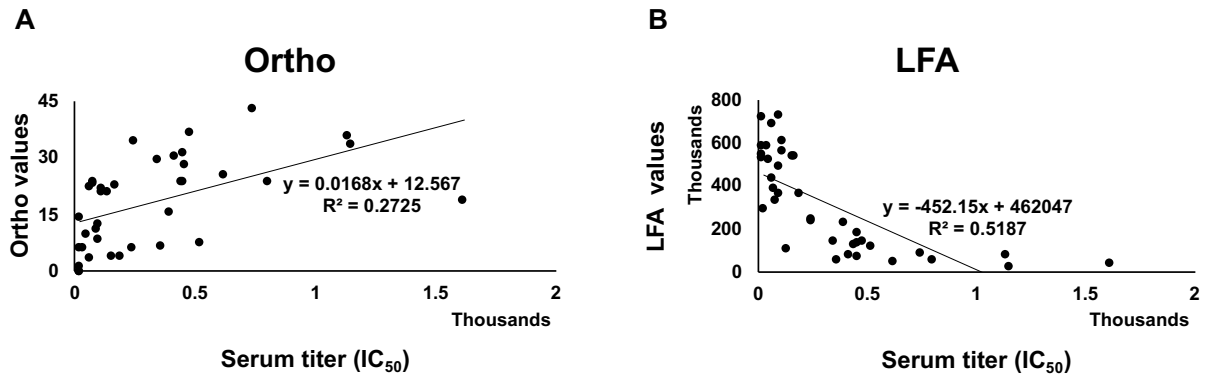

Figure 4. Regression analysis between **(A)** LFA and serum titer, and **(B)** Ortho Vitros SARS-CoV-2 IgG test and titer. Regression plots show explained variance (R^2) between compared methods. Thirty-eight samples were tested.

LFA values accounted for roughly 52% of observed variance in IC_{50} values, while Ortho Vitros Anti-SARS-CoV-2 IgG test accounted for approximately 27% of IC_{50} variance. Since the format of the LFA reports decreasing density values as neutralization increases, LFA was significantly inversely correlated with IC_{50} values (r = -0.720, p < 0.001), while Ortho Vitros Anti-SARS-CoV-2 IgG test values showed a significant positive correlation to IC_{50} values (r = 0.522, p = 0.001). Additionally, LFA and Ortho Vitros Anti-SARS-CoV-2 IgG test values showed a significant relationship with each other (r = -0.572, p < 0.001).

To evaluate bias between the assays, mean differences and 95% confidence intervals (CIs) were calculated and plotted alongside limits of agreement (**Figure 5**). Both LFA and Ortho Vitros Anti-SARS-CoV-2 IgG test values showed high agreement with titer, although Ortho Vitros Anti-SARS-CoV-2 IgG test showed a tendency to underestimate neutralizing capacity while the LFA method showed no bias.

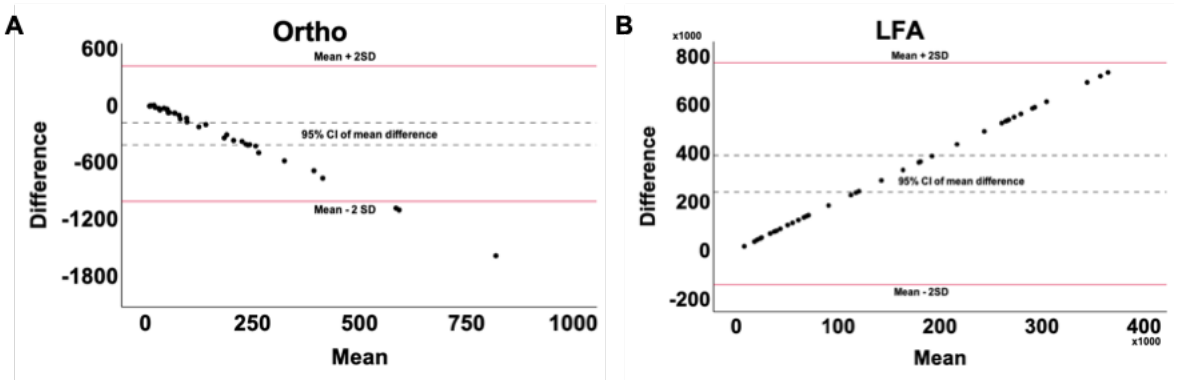

Figure 5. Bland-Altman plots showing bias (mean difference and 95% CI) and computed limits of agreement (mean difference ± 2SD) between **(A)** Ortho Vitros Anti-SARS-CoV-2 IgG test and IC_{50} values and **(B)** our LFA and IC_{50} values. Thirty-eight samples were tested.

Univariate ROC analysis was performed to assess the performance of the newly developed LFA and Ortho assay to classify non-neutralizing (Neg—1:160), and neutralizing groups (≥1:320) (**Figure 6**). As can be seen in **Figure 6B** and **6D**, the LFA misclassified one non-neutralizing sample (Neg—1:160) as neutralizing (≥1:320). In contrast, Ortho Vitros Anti-SARS-CoV-2 IgG test misclassified that same non-neutralizing sample as neutralizing, in addition to incorrectly classifying five additional neutralizing samples as non-neutralizing. Importantly, our LFA method exhibited a greater dynamic range of differential values as compared to Ortho's test. (**Figure 5**), translating to superior classification accuracy of the LFA method in detecting neutralizing samples (titer ≥ 1:320) compared to Ortho Vitros Anti-SARS-CoV-2 IgG test (**Figures 6A** and **6C**).

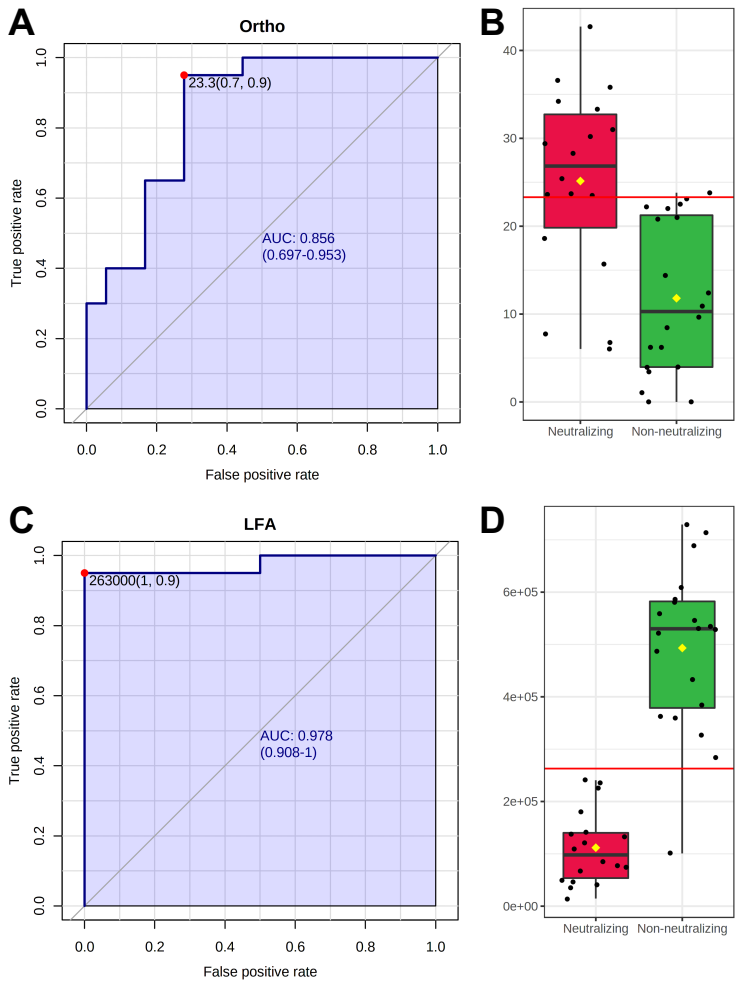

Figure 6. **(A)** Univariate ROC analysis of Ortho Vitros Anti-SARS-CoV-2 IgG test for discrimination of neutralizing samples (≥1:320) [AUC: 0.856, 95% CI: 0.697—0.953, sensitivity = 0.7, specificity = 0.9]. **(B)** Box plot of Ortho Vitros Anti-SARS-CoV-2 IgG test values between neutralizing (≥1:320) and non-neutralizing (Neg—1:160) groups. **(C)** Univariate ROC analysis of LFA for discrimination of neutralizing samples (≥1:320) [AUC: 0.978, 95% CI: 0.908—1.0, sensitivity = 1.0, specificity = 0.9]. **(D)** Box plot of LFA values between neutralizing (≥1:320) and non-neutralizing (Neg—1:160) groups.

Our LFA showed high accuracy for classification of neutralizing samples (AUC = 0.978), while the Ortho Vitros Anti-SARS-CoV-2 IgG test showed modest accuracy for classification of neutralizing samples (AUC = 0.856). Furthermore, while the LFA method showed a narrow confidence interval (95% CI: 0.908—1.00), ROC analysis of Ortho Vitros Anti-SARS-CoV-2 IgG test values showed a wider range (95% CI: 0.697—0.953), indicating less certainty. Notably, while both methods showed roughly 90% specificity, Ortho Vitros Anti-SARS-CoV-2 IgG test Vitros Anti-

363 SARS-CoV-2 IgG test showed only 70% sensitivity. In contrast, the novel LFA method showed
364 perfect sensitivity (100%) in this analysis of 38 samples.

365 Optimal cutoffs were computed to maximize AUC. For the LFA, density unit values below
366 263,000 classify samples as neutralizing and correspond to titers ≥1:320. Density unit values
367 above this LFA cutoff classify samples in the non-neutralizing group. For the Ortho Vitros Anti-
368 SARS-CoV-2 IgG test, values between 0 and 23.3 were representative of non-neutralizing
369 capacity, whereas values above 23.3 were reflective of the neutralizing group. If we used the
370 FDA cutoff of 12 instead of the 23.3 value calculated using our results, AUC would be reduced to
371 0.69 (sensitivity = 0.55, specificity = 0.83).

372 Polyclonal antisera was used in this study, not an individual Mab, so the limit of detection
373 (LoD) does not exactly apply). However, we can calculate the LoD by line density based on the
374 method of Armbruster and Pry(26) as the highest line density from samples still containing
375 neutralizing antibodies and distinguishable from blank except that the operand sign was changed
376 because due to the competitive format of the LFA: LoD= limit of blank (LoB) – (1.65* $SD_{low\ conc}$
377 $_{sample}$): LoD=1,047,382- (1.65 * 63,769)= 942,481 Test Line Density Units. The average line
378 density observed for the top 10 donors who demonstrated the strongest ability to prevent RBD
379 from binding to ACE2 was 20,706.

380 The principle of infusing convalescent plasma from recovered individuals into patients
381 fighting COVID-19 is to transfer NAbs from the donor to the recipient, as has been done for
382 several other diseases(27–29). The rapid test described here, could quickly and efficiently
383 classify COVID-19 convalescent plasma (CCP) units so that the sickest patients might receive
384 the most potently neutralizing plasma. Although levels of neutralizing antibody to achieve in
385 patients receiving CCP remains undefined, our point-of-care test might be useful at the bedside
386 to monitor a patient receiving highly neutralizing CCP as he/she begins to demonstrate NAbs in
387 circulation, as shown in **Figure 7A**. It could help in deciding whether to administer another unit

388 of highly neutralizing CCP to a patient fighting COVID19. The same scenario might also be
389 applied to hyperimmune gammaglobulin or neutralizing monoclonal antibody infusion.
390 To demonstrate the utility of our LFA to measure NAbs in whole blood, we used a lateral
391 flow strip with a blood filter and performed an experiment in which a neutralizing monoclonal
392 antibody based on the B-38(20) sequence was titrated into whole blood as shown in **Figure 7B**.
393 Density units were not obtained in these experiments but both **Figures 7A** and **7B** demonstrate
394 the semi-quantitative nature of this test to visually distinguish different levels of NAbs in plasma
395 and whole blood.
396

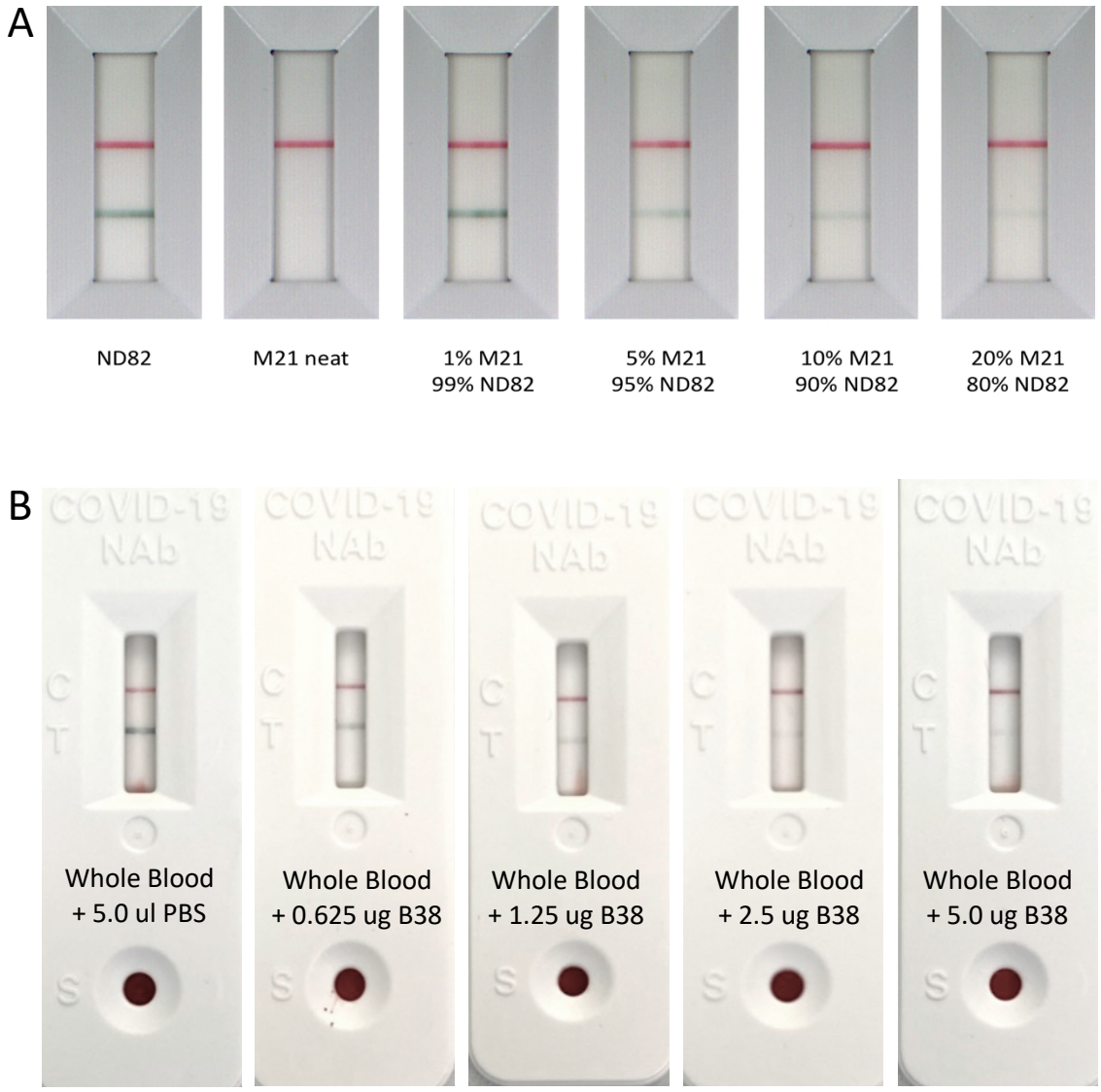

Figure 7. (A) Highly neutralizing plasma from an individual recovered from COVID-19 (M21) converts non-immune human plasma (ND82) into highly neutralizing plasma; 10µl of plasma was added to each lateral flow cassette. Text below each lateral flow cassette indicates the percent M21 and percent ND82 plasma used to run the lateral flow test. **(B)** Titration of anti-RBD neutralizing mAb into 10µl of heparinized whole blood. For both types of cassettes, plasma or blood sample was immediately chased with 50µl sample buffer. Densities were read and cassettes were imaged after 10 minutes development.

Discussion

Serologic tests that detect responses to infection are an important population surveillance tool during pandemics because they provide data on pathogen exposure, especially

441 when a subset of the population is asymptomatic and would not have been diagnosed by
442 molecular methods(30, 31). While over 90% of individuals diagnosed with COVID-19 generate
443 antibody responses(30) we are only beginning to learn about the prevalence and duration of
444 NAbs induced by a natural infection. This lack of knowledge is mainly due to the fact that virus-
445 based neutralization assays require *i)* BSL2 or BSL3 facilities, *ii)* highly skilled personnel, *iii)*
446 permissive cells and quantified virus, and *iv)* take longer than 24 hours to obtain results. Since
447 every viral vaccine, including COVID-19 vaccines, administered to humans is designed to elicit
448 antibodies that neutralize virus by blocking host cell infection, development of NAbs is a
449 hallmark of protection from disease. Therefore, there is a need for rapid, accurate tests that
450 measure levels of NAbs. Furthermore, in a post-vaccine world, longitudinal measurement of
451 protective, neutralizing antibodies is crucial. Measurement of anti-viral T cells also indicates that
452 infected individuals could destroy infected host cells if virus escapes neutralization.
453 We developed a rapid, 10-minute lateral flow test that measures levels of NAbs in serum
454 and plasma. As shown in **Figure 2**, the lateral flow test correlates well with serologic titers
455 determined using a VSV-based pseudotype assay, and IC_{50} values in an authentic SARS-CoV-2
456 microneutralization assay, especially when serum sample titers are ≥640 and IC_{50} values
457 are >250. Samples with less potent NAbs in both viral assays correlated with decreased ability
458 to block RBD from binding to ACE2 in the LFAs.
459 The LFA and Ortho Vitros Anti-SARS-CoV-2 IgG test methods showed a strong,
460 significant correlation with each other (r = -0.572, p < 0.001), displaying an appreciable degree of
461 linear relation (r = -0.720, p < 0.001)(32). Importantly, LFA accounts for 52% of observed IC_{50}
462 variance (R^2 = 0.5187) while, in comparison, Ortho Vitros Anti-SARS-CoV-2 IgG test accounts for
463 27% (R^2 = 0.2725). Although absolute quantitation of a construct demands an excellent coefficient
464 of determination (R^2 ≥ 0.99)(33), variables with R^2 ≥ 0.5 are highly predictive in univariate
465 regression models while measures with R^2 < 0.5 are recommended for use in multivariate models
466 in combination with complementary measures to increase predictive accuracy(34, 35).

Additionally, Bland-Altman analysis (**Figure 5**) showed the Ortho Vitros Anti-SARS-CoV-2 IgG test to be prone to underestimation of IC_{50} values. In contrast, the LFA method did not exhibit any over- or underestimation bias. Furthermore, across mean values for both methods, LFA showed discrete differential values while Ortho Vitros Anti-SARS-CoV-2 IgG test struggled to differentiate samples with high neutralizing capacity (IC_{50} values).

Since the Ortho Vitros Anti-SARS-CoV-2 IgG test uses S1, which includes RBD, it is likely that antibodies reactive with other parts of S1–even some that may neutralize via N-terminal domain–are responsible for increased reactivity to S1 when they are not neutralizing in our RBD-ACE2 competition assay. Advantages of our POC test is that it can be inexpensively and rapidly deployed in studies to determine levels of NAbs that protect against re-infection and limit transmission of the virus. Moreover, rapid inexpensive tests can be used longitudinally to evaluate duration of protective immunity in both naturally infected and many more vaccinated individuals than could ever be evaluated using BSL2 or BSL3-based neutralization assays.

In the setting of much debated CCP, a rapid test could be used to measure levels of NAbs in a CCP product prior to infusion, or potential donors who recovered from COVID-19. During infusion of CCP, a rapid test could be used to help decide if a patient fighting COVID-19 requires another unit of highly neutralizing plasma. If a particular donor's CCP has very high levels of CCP, patients might need only one unit. On the other hand, if donor CCP contains moderate levels of NAbs, the patient may require multiple units to achieve therapeutic levels of NAbs. However, since we do not know what an adequate therapeutic dose of NAbs is, this rapid test could be a valuable tool in trials to determine under what conditions CCP, hyperimmune globulin, and neutralizing mAbs are effective therapeutic agents for COVID19 patients.

493 Limitations of the LFA are that it uses only the RBD portion of SARS-CoV-2 spike
494 protein. Although the vast majority of reports indicate that the principle neutralizing domain is
495 RBD portion of spike protein, mAbs have been reported that neutralize SARS-CoV-2 by binding
496 to the N-terminal domain of spike protein(36, 37). Also, since the spike protein assumes several
497 conformations during viral binding and entry(38), neutralizing epitopes exist on the quaternary
498 structure of spike(37). Although RBDs on the nanoparticles may associate, it is unlikely they
499 assume a native quaternary conformation.
500 Other limitations are the binary nature of the data analysis (neutralizing and non-
501 neutralizing) of a continuous assay. Clearly, line densities demonstrate moderate levels of
502 neutralization. Since blood draws and subsequent assays are a “snapshot in time” of
503 neutralizing antibody activity, levels were undoubtedly increasing in some patients and
504 decreasing in others. LFAs are generally inexpensive and highly portable compared to other
505 laboratory-based tests, so neutralizing antibody levels could be measured using the LFA to
506 longitudinally assess protective neutralizing antibody immunity. Another limitation is that the
507 LFA does not differentiate high affinity anti-RBD NAbs from an abundance of lower affinity anti-
508 RBD NAbs. In related experiments, we have observed patient sera that bind strongly to RBD,
509 but do not demonstrate neutralizing activity (data not shown).
510 This test may prove very useful in monitoring COVID-19 vaccine recipients. Although
511 vaccines have now been approved for distribution and administration, durability of protective
512 immunity elicited by any COVID-19 vaccine is unknown. It is the goal of all COVID-19 vaccines
513 to induce protective NAbs. However, since clinical trials of vaccines have enrolled 30,000 to
514 60,000 participants, it is not logistically possible to draw a tube of blood from each vaccine
515 recipient longitudinally to determine duration of protective NAbs. Application of our test in
516 vaccine recipients using a drop of blood obtained from a finger-stick as shown in **Figure 7B**
517 might lead to more comprehensive longitudinal monitoring of increases and decreases in
518 protective humoral immunity.

519

520 **Data availability**

521 The authors declare that data supporting the findings of this study are available within the
522 paper. Additional data mentioned but not shown are available from the corresponding author
523 upon reasonable request.

524

525 **References**

526 1. Ghinai I, McPherson TD, Hunter JC, Kirking HL, Christiansen D, Joshi K, Rubin R, Morales-Estrada S,
527 Black SR, Pacilli M, Fricchione MJ, Chugh RK, Walblay KA, Ahmed NS, Stoecker WC, Hasan NF,
528 Burdsall DP, Reese HE, Wallace M, Wang C, Moeller D, Korpics J, Novosad SA, Benowitz I, Jacobs
529 MW, Dasari VS, Patel MT, Kauerauf J, Charles EM, Ezike NO, Chu V, Midgley CM, Rolfes MA, Gerber
530 SI, Lu X, Lindstrom S, Verani JR, Layden JE, Brister S, Goldesberry K, Hoferka S, Jovanov D, Nims D,
531 Saathoff-Huber L, Hoskin Snelling C, Adil H, Ali R, Andreychak E, Bemis K, Frias M, Quartey-
532 Kumapley P, Baskerville K, Murphy E, Murskyj E, Noffsinger Z, Vercillo J, Elliott A, Onwuta US, Burck
533 D, Abedi G, Burke RM, Fagan R, Farrar J, Fry AM, Hall AJ, Haynes A, Hoff C, Kamili S, Killerby ME,
534 Kim L, Kujawski SA, Kuhar DT, Lynch B, Malapati L, Marlow M, Murray JR, Rha B, Sakthivel SKK,
535 Smith-Jeffcoat SE, Soda E, Wang L, Whitaker BL, Uyeki TM. 2020. First known person-to-person
536 transmission of severe acute respiratory syndrome coronavirus 2 (SARS-CoV-2) in the USA. The
537 Lancet 395:1137–1144.

538 2. Huang C, Wang Y, Li X, Ren L, Zhao J, Hu Y, Zhang L, Fan G, Xu J, Gu X, Cheng Z, Yu T, Xia J, Wei Y, Wu
539 W, Xie X, Yin W, Li H, Liu M, Xiao Y, Gao H, Guo L, Xie J, Wang G, Jiang R, Gao Z, Jin Q, Wang J, Cao
540 B. 2020. Clinical features of patients infected with 2019 novel coronavirus in Wuhan, China. The
541 Lancet 395:497–506.

3. Li R, Pei S, Chen B, Song Y, Zhang T, Yang W, Shaman J. 2020. Substantial undocumented infection facilitates the rapid dissemination of novel coronavirus (SARS-CoV-2). Science 368:489–493.

4. Widge AT, Rouphael NG, Jackson LA, Anderson EJ, Roberts PC, Makhene M, Chappell JD, Denison MR, Stevens LJ, Pruijssers AJ, McDermott AB, Flach B, Lin BC, Doria-Rose NA, O'Dell S, Schmidt SD, Neuzil KM, Bennett H, Leav B, Makowski M, Albert J, Cross K, Edara V-V, Floyd K, Suthar MS, Buchanan W, Luke CJ, Ledgerwood JE, Mascola JR, Graham BS, Beigel JH. 2020. Durability of Responses after SARS-CoV-2 mRNA-1273 Vaccination. N Engl J Med 4.

5. Loeffelholz MJ, Tang Y-W. 2020. Laboratory diagnosis of emerging human coronavirus infections – the state of the art. Emerg Microbes Infect 9:747–756.

6. Yongchen Z, Shen H, Wang X, Shi X, Li Y, Yan J, Chen Y, Gu B. 2020. Different longitudinal patterns of nucleic acid and serology testing results based on disease severity of COVID-19 patients. Emerg Microbes Infect 9:833–836.

7. McAndrews KM, Dowlatshahi DP, Hensel J, Ostrosky-Zeichner LL, Papanna R, LeBleu VS, Kalluri R. 2020. Identification of IgG antibody response to SARS-CoV-2 spike protein and its receptor binding domain does not predict rapid recovery from COVID-19. preprint, Infectious Diseases (except HIV/AIDS).

8. Han Z, Battaglia F, Terlecky SR. 2020. Discharged COVID-19 Patients Testing Positive Again for SARS-CoV-2 RNA: A Minireview of Published Studies from China. J Med Virol jmv.26250.

9. Ye G, Pan Z, Pan Y, Deng Q, Chen L, Li J, Li Y, Wang X. 2020. Clinical characteristics of severe acute respiratory syndrome coronavirus 2 reactivation. J Infect 80:e14–e17.

562 10. Hoang VT, Dao TL, Gautret P. 2020. Recurrence of positive SARS-CoV-2 in patients recovered from
563 COVID-19. J Med Virol jmv.26056.

564 11. Robbiani DF, Gaebler C, Muecksch F, Lorenzi JCC, Wang Z, Cho A, Agudelo M, Barnes CO, Gazumyan
565 A, Finkin S, Hagglof T, Oliveira TY, Viant C, Hurley A, Hoffmann H-H, Millard KG, Kost RG, Cipolla M,
566 Gordon K, Bianchini F, Chen ST, Ramos V, Patel R, Dizon J, Shimeliovich I, Mendoza P, Hartweger H,
567 Nogueira L, Pack M, Horowitz J, Schmidt F, Weisblum Y, Michailidis E, Ashbrook AW, Waltari E, Pak
568 JE, Huey-Tubman KE, Koranda N, Hoffman PR, West AP, Rice CM, Hatziioannou T, Bjorkman PJ,
569 Bieniasz PD, Caskey M, Nussenzweig MC. 2020. Convergent Antibody Responses to SARS-CoV-2
570 Infection in Convalescent Individuals. preprint, Immunology.

571 12. Juno JA, Tan H-X, Lee WS, Reynaldi A, Kelly HG, Wragg K, Esterbauer R, Kent HE, Batten CJ, Mordant
572 FL, Gherardin NA, Pymm P, Dietrich MH, Scott NE, Tham W-H, Godfrey DI, Subbarao K, Davenport
573 MP, Kent SJ, Wheatley AK. 2020. Immunogenic profile of SARS-CoV-2 spike in individuals recovered
574 from COVID-19. preprint, Infectious Diseases (except HIV/AIDS).

575 13. Wu F, Wang A, Liu M, Wang Q, Chen J, Xia S, Ling Y, Zhang Y, Xun J, Lu L, Jiang S, Lu H, Wen Y, Huang
576 J. 2020. Neutralizing antibody responses to SARS-CoV-2 in a COVID-19 recovered patient cohort
577 and their implications. MedRxiv Prepr 20.

578 14. Vandergaast R, Carey T, Reiter S, Lech P, Gnanadurai C, Tesfay M, Buehler J, Suksanpaisan L, Naik S,
579 Brunton B, Recker J, Haselton M, Ziegler C, Roesler A, Mills JR, Theel E, Weaver SC, Rafael G,
580 Roforth MM, Jerde C, Tran S, Diaz RM, Bexon A, Baum A, Kyratsous CA, Peng KW, Russell SJ. 2020.
581 Development and validation of IMMUNO-COV™: a high-throughput clinical assay for detecting
582 antibodies that neutralize SARS-CoV-2. preprint, Immunology.

15. Crawford KHD, Eguia R, Dingens AS, Loes AN, Malone KD, Wolf CR, Chu HY, Tortorici MA, Veesler D, Murphy M, Pettie D, King NP, Balazs AB, Bloom JD. 2020. Protocol and reagents for pseudotyping lentiviral particles with SARS-CoV-2 Spike protein for neutralization assays. preprint, Microbiology.

16. Wang Q, Zhang Y, Wu L, Niu S, Song C, Zhang Z, Lu G, Qiao C, Hu Y, Yuen K-Y, Wang Q, Zhou H, Yan J, Qi J. 2020. Structural and Functional Basis of SARS-CoV-2 Entry by Using Human ACE2. Cell S009286742030338X.

17. Premkumar L, Segovia-Chumbez B, Jadi R, Martinez DR, Raut R, Markmann A, Cornaby C, Bartelt L, Weiss S, Park Y, Edwards CE, Weimer E, Scherer EM, Rouphael N, Edupuganti S, Weiskopf D, Tse LV, Hou YJ, Margolis D, Sette A, Collins MH, Schmitz J, Baric RS, de Silva AM. 2020. The receptor binding domain of the viral spike protein is an immunodominant and highly specific target of antibodies in SARS-CoV-2 patients. Sci Immunol 5:eabc8413.

18. Tan CW, Chia WN, Qin X, Liu P, Chen MI-C, Tiu C, Hu Z, Chen VC-W, Young BE, Sia WR, Tan Y-J, Foo R, Yi Y, Lye DC, Anderson DE, Wang L-F. 2020. A SARS-CoV-2 surrogate virus neutralization test based on antibody-mediated blockage of ACE2–spike protein–protein interaction. Nat Biotechnol https://doi.org/10.1038/s41587-020-0631-z.

19. Hanson QM, Wilson KM, Shen M, Itkin Z, Eastman RT, Shinn P, Hall MD. 2020. Targeting ACE2-RBD interaction as a platform for COVID19 therapeutics: Development and drug repurposing screen of an AlphaLISA proximity assay. preprint, Biochemistry.

20. Wu Y, Wang F, Shen C, Peng W, Li D, Zhao C, Li Z, Li S, Bi Y, Yang Y, Gong Y, Xiao H, Fan Z, Tan S, Wu G, Tan W, Lu X, Fan C, Wang Q, Liu Y, Zhang C, Qi J, Gao GF, Gao F, Liu L. 2020. A noncompeting pair of human neutralizing antibodies block COVID-19 virus binding to its receptor ACE2. Science 368:1274–1278.

605 21. Davide Giavarina. 2015. Understanding Bland Altman analysis. Biochem Medica 25:141–151.

606 22. Doğan NÖ. 2018. Bland-Altman analysis: A paradigm to understand correlation and agreement. Turk
607 J Emerg Med 18:139–141.

608 23. Obuchowski NA, Bullen JA. 2018. Receiver operating characteristic (ROC) curves: review of methods
609 with applications in diagnostic medicine. Phys Med Biol 29.

610 24. Nakas CT, Yannoutsos CT. November 30. Ordered multiple-class ROC analysis with continuous
611 measurements. Med Stat 23:3437–49.

612 25. Xie X, Muruato A, Lokugamage KG, Narayanan K, Zhang X, Zou J, Liu J, Schindewolf C, Bopp NE,
613 Aguilar PV, Plante KS, Weaver SC, Makino S, LeDuc JW, Menachery VD, Shi P-Y. 2020. An Infectious
614 cDNA Clone of SARS-CoV-2. Cell Host Microbe 27:841-848.e3.

615 26. Armbruster DA, Pry T. Limit of Blank, Limit of Detection and Limit of Quantitation. 2008 Clin
616 Biochem Rev 29:s50.

617 27. Leider JP, Brunker PAR, Ness PM. 2010. Convalescent transfusion for pandemic influenza: preparing
618 blood banks for a new plasma product?: CONVALESCENT TRANSFUSION FOR PANDEMIC
619 INFLUENZA. Transfusion (Paris) 50:1384–1398.

620 28. Yeh K-M, Chiueh T-S, Siu LK, Lin J-C, Chan PKS, Peng M-Y, Wan H-L, Chen J-H, Hu B-S, Perng C-L, Lu J-
621 J, Chang F-Y. 2005. Experience of using convalescent plasma for severe acute respiratory syndrome
622 among healthcare workers in a Taiwan hospital. J Antimicrob Chemother 56:919–922.

623 29. Enria D, Briggiler A, Fernandez N, Levis S, Maiztegui J. 1984. Importance of dose of neutralising
624 antibodies in treatment of Agentine Haemorrhagic Fever with immune plasma. The Lancet 255–
625 256.

626 30. Gudbjartsson DF, Norddahl GL, Melsted P, Gunnarsdottir K, Holm H, Eythorsson E, Arnthorsson AO,
627 Helgason D, Bjarnadottir K, Ingvarsson RF, Thorsteinsdottir B, Kristjansdottir S, Birgisdottir K,
628 Kristinsdottir AM, Sigurdsson MI, Arnadottir GA, Ivarsdottir EV, Andresdottir M, Jonsson F,
629 Agustsdottir AB, Berglund J, Eiriksdottir B, Fridriksdottir R, Gardarsdottir EE, Gottfredsson M,
630 Gretarsdottir OS, Gudmundsdottir S, Gudmundsson KR, Gunnarsdottir TR, Gylfason A, Helgason A,
631 Jensson BO, Jonasdottir A, Jonsson H, Kristjansson T, Kristinsson KG, Magnusdottir DN, Magnusson
632 OT, Olafsdottir LB, Rognvaldsson S, le Roux L, Sigmundsdottir G, Sigurdsson A, Sveinbjornsson G,
633 Sveinsdottir KE, Sveinsdottir M, Thorarensen EA, Thorbjornsson B, Thordardottir M,
634 Saemundsdottir J, Kristjansson SH, Josefsdottir KS, Masson G, Georgsson G, Kristjansson M, Moller
635 A, Palsson R, Gudnason T, Thorsteinsdottir U, Jonsdottir I, Sulem P, Stefansson K. 2020. Humoral
636 Immune Response to SARS-CoV-2 in Iceland. N Engl J Med NEJMoa2026116.

637 31. Lee S, Kim T, Lee E, Lee C, Kim H, Rhee H, Park SY, Son H-J, Yu S, Park JW, Choo EJ, Park S, Loeb M,
638 Kim TH. 2020. Clinical Course and Molecular Viral Shedding Among Asymptomatic and
639 Symptomatic Patients With SARS-CoV-2 Infection in a Community Treatment Center in the
640 Republic of Korea. JAMA Intern Med https://doi.org/10.1001/jamainternmed.2020.3862.

641 32. Schober P, Boer C, Schwarte LA. 2018. Correlation Coefficients: Appropriate Use and Interpretation.
642 Anesth Analg 126:1763–1768.

643 33. Rights JD, Sterba SK. Quantifying explained variance in multilevel models: An integrative framework
644 for defining R-squared measures. Psychol Methods 24:309–338.

645 34. Rights JD, Sterba SK. A framework of R-squared measures for single-level and multilevel regression
646 mixture models. Psychol Methods 23:434–457.

647 35. Rights JD, Sterba SK. New Recommendations on the Use of R-Squared Differences in Multilevel
648 Model Comparisons. Multivar Behav Res 55:568–599.

649 36. Chi X, Yan R, Zhang J, Zhang G, Zhang Y, Hao M, Zhang Z, Fan P, Dong Y, Yang Y, Chen Z, Guo Y, Zhang
650 J, Li Y, Song X, Chen Y, Xia L, Fu L, Hou L, Xu J, Yu C, Li J, Zhou Q, Chen W. 2020. A neutralizing
651 human antibody binds to the N-terminal domain of the Spike protein of SARS-CoV-2. Science
652 eabc6952.

653 37. Liu L, Wang P, Nair MS, Yu J, Rapp M, Wang Q, Luo Y, Chan JF-W, Sahi V, Figueroa A, Guo XV, Cerutti
654 G, Bimela J, Gorman J, Zhou T, Chen Z, Yuen K-Y, Kwong PD, Sodroski JG, Yin MT, Sheng Z, Huang Y,
655 Shapiro L, Ho DD. 2020. Potent neutralizing antibodies against multiple epitopes on SARS-CoV-2
656 spike. Nature 584:450–456.

657 38. Cai Y, Zhang J, Xiao T, Peng H, Sterling SM, Walsh RM, Rawson S, Rits-Volloch S, Chen B. 2020.
658 Distinct conformational states of SARS-CoV-2 spike protein. Science eabd4251.

659
660
661
662
663
664
665

666
667
668

669
670
671